Comparative study of Y and other transition metals on GaAs(110)

F. Schäffler, G. Hughes,* W. Drube, R. Ludeke, and F. J. Himpsel
IBM Thomas J. Watson Research Center, P.O. Box 218, Yorktown Heights, New York 10598
(Received 13 November 1986)

Interface chemistry and Schottky-barrier formation of Y/GaAs interfaces are studied by high-resolution photoemission (PES) and inverse-photoemission (IPES) spectroscopies and are compared with results from other transition metals on cleaved GaAs surfaces. As with all other transition metals studied so far, the interface chemistry is characterized by a heavily reacted layer, which involves both Ga and As atoms. Ga diffuses into the overlayer, while As stays close to the interface, in contrast to the inverse behavior found in many other transition-metal—GaAs systems. Contrary to, e.g., Ti or V, the PES and IPES spectra of Y overlayers show at low coverages no *d*-electron-related filled or empty states in the band gap of GaAs. The direct involvement of rehybridized *d*-electron states in the Fermi-level pinning, that has been proposed for several other transition metals, can be ruled out at least for the Y/*p*-type-GaAs interface. Alternative mechanisms responsible for the observed Schottky barrier are discussed. The variation of the barrier height with coverage indicates an influence of the metallic properties of the overlayer on the final Fermi-level pinning position. This applies especially for *n*-type GaAs, for which the final barrier height is not established before the overlayer reaches a thickness of ≥ 10 Å. The variation of the band bending with coverage suggests a change in the energetic distribution of acceptor states with increasing Y coverage.

I. INTRODUCTION

The characterization of the microscopic mechanisms leading to the formation of Schottky barriers on III-V compound semiconductors has always suffered from a lack of sensitivity both at low metal coverages, for which the density of interface states necessary for Fermi-level pinning is only of the order of 10^{12} cm^{-2}, and at higher coverages, for which the metal conduction band overlaps the semiconductor valence band and part of the intrinsic band gap. Consequently, photoemission spectroscopy (PES) experiments were until recently not able to provide spectroscopic evidence for these bandgap states and their energetic distribution. Therefore, all models proposed for the Schottky-barrier-formation mechanism are either based on theoretical results,[1-4] or on the interpretation of indirect experiments.[5-7] An example of the latter is the variation of the Fermi-level pinning position within the bandgap as a function of adsorbate coverage, which can usually be fitted by one pair of effective donor and acceptor levels, but with a substantial ambiguity in their respective energy levels.[8] Novel techniques[9,10] will most likely play an important role in direct spectroscopy of interface states in the near future, but at present, only limited data are available. Another approach was recently chosen by Ludeke *et al.*[11,12] who studied transition metals on cleaved III-V compound semiconductor surfaces with conventional PES techniques. These experiments were based on the relatively large scattering cross-section of *d* electrons and the fact that several transition metals have been identified as deep traps in the bulk of both group-IV elemental and III-V compound semiconductors. The latter aspect is of substantial technological importance (e.g., Cr or V doping of GaAs in the production of semi-insulating substrate material), and has led to a large variety of theoretical[13,14] and experimental[15-17] papers on that subject. Therefore, it is well known that a transition metal impurity usually substitutes a group-III atom (cation) in a III-V semiconductor lattice, which causes a rehybridization of the *d* electrons. The tetrahedral crystal field leads to a splitting of the *d* band into bonding and empty or partly filled antibonding and nonbonding levels. Depending on the energetic position of these levels with respect to the intrinsic band gap and on the charge state of the substitutional impurity, such a state can act as donor and/or acceptor. Little is known so far about possible corrections for these energy states as the impurity is moved to the surface or to a metal-semiconductor interface, which reduces the symmetry of the problem. However, since the precision of theoretically predicted impurity levels is of the order of the bandgap itself, present theories are at best capable of giving trends rather than predicting reliable absolute energy values. In addition, the reactivity of most of the transition metals suggests that not only substitutional cation defects but also more complicated defect complexes are created when evaporating transition metals on clean semiconductor surfaces. Hence, it appears necessary to study several transition-metal—semiconductor interfaces individually with the aim of establishing chemical trends for their relevance in the Schottky-barrier-formation process.

So far, detailed Schottky-barrier studies have been published for Ti($3d^2 4s^2$ configuration), Pd($4d^{10} 5s^2$), V($3d^3 4s^2$), and Mn($3d^5 4s^2$) on *n*- and *p*-type GaAs,[11,12] with the latter two metals also reported on InP.[18] In all these systems *d*-electron-related emission was observed in the intrinsic semiconductor band gap up to the Fermi level for coverages well below the formation of a metallic overlayer. This finding provides strong evidence for the

 ©1987 The American Physical Society

direct involvement of transition metal impurities in the Schottky-barrier-formation mechanism and was recently supported by inverse photoemission results for some of these interfaces, which showed empty states in the bandgap down to the Fermi level.[19,20] All four transition metals mentioned have more than three valence electrons, which means that they can act—in principle—as donor and acceptor states, since the neutral charge state at a substitutional cation site is 3 + . In the following, we present PES and IPES (inverse PES) results of Y on GaAs, which is particularly interesting, since the $4d^1 5s^2$ configuration of Y is not expected to produce a donor state at a substitutional cation site, as all three valence electrons are involved in the chemical bonding. The differences in chemistry and Fermi-level pinning are illustrated by comparing these results with experiments of other transition-metal interfaces.

II. PHOTOEMISSION AND INVERSE PHOTOEMISSION EXPERIMENTS

All PES experiments were performed at the vuv ring of the National Synchrotron Light Source (NSLS) at Brookhaven National Laboratory (Upton, N.Y.). The 6-m toroidal grating monochromator and the two-dimensional (2D) display analyzer, which was used in an angle-integrating mode, have been described elsewhere.[21] Normal-emission IPES measurements were performed in a special spectrometer using a grating monochromator and multichannel detection of the photon spectrum.[22] GaAs single crystals with a Si (*n*-type) doping concentration of 2×10^{17} cm^{-3}, and Zn (*p*-type) doping of $(5-10)\times10^{17}$ cm^{-3} were preoriented and cut in bars of 3×3 mm^2 cross section in the (110) cleavage plane. The samples were cleaved *in situ* and tested for flatband condition; only cleaves with an initial band bending of less than 150 mV were used for further experiments. High-purity Y was evaporated from Y ribbons, which were heated by an electron-beam or direct resistive heating. After careful outgasing of the sources, the system pressure could be kept in the middle 10^{-10} Torr range during evaporation, up from a base pressure of $\simeq10^{-10}$ Torr. Evaporation rates were calibrated with a quartz-crystal monitor and checked before and after each evaporation. Rates were adjusted between 10^{-3} and 5×10^{-2} Å/sec, with the higher ones used at coverages exceeding 1 Å. All evaporations and measurements were carried out with the cleaved sample held at room temperature. Coverages are given in units of angströms, with an equivalent monolayer [defined as 8.85×10^{14} atoms/cm^2, the atomic density of a GaAs (110) layer] of Y, V, Ti, and Pd corresponding to a thickness of 2.95, 1.26, 1.56, and 1.30 Å, respectively. Note that an equivalent monolayer (ML) of Y is up to two times thicker than for the other transition metals discussed. Core-level spectra were taken in a surface-sensitive mode by choosing appropriate photon energies to achieve minimal electron escape depths (≤ 5Å). The bandpass of the analyzer was set to give an estimated combined resolution of monochromator and analyzer of ≤ 200 meV for core-level spectra, and ≤ 400 meV for valence band spectra. The energy resolution of the IPES spectra is estimated to be 300 meV. The digitally recorded core-level spectra were decomposed into their respective spin-orbit-split components by means of a computer routine described in detail elsewhere.[23] In brief, the least-square routine minimizes the difference between the actual spectrum and a synthesized one, which is generated from spin-orbit-split Lorentzian doublets broadened by a Gaussian line shape, the latter accounting for instrumental broadening as well as for inhomogeneities in chemical phase and band bending. The number of adjustable parameters is kept minimal by determining spin-orbit splitting and the intensity ratio between the spin-orbit-split components from the spectra of the clean sample, and keeping these constant for all coverages and chemically shifted components.

A. Interface chemistry

Figure 1 shows the evolution of the As 3*d* and Ga 3*d* core levels as a function of Y coverage. The dots represent the data after subtraction of a smooth background, while the solid lines show the fitted components.

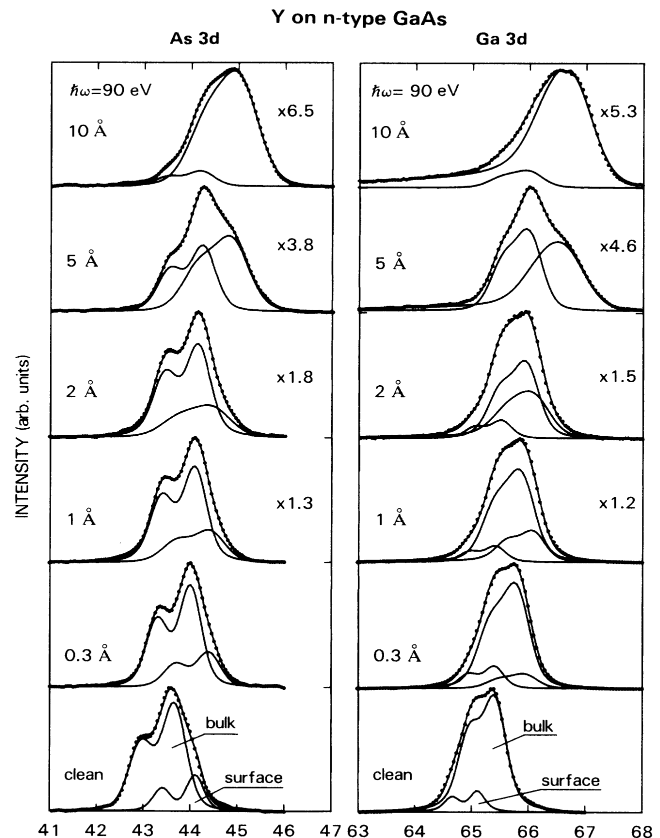

FIG. 1. PES spectra of the Ga 3*d* and As 3*d* core levels for increasing Y coverage at a photon energy of 90 eV. The data (dots) are decomposed into bulk, surface, and reacted components. Their sum is represented by the line through the data points. The attenuation of the core-level signals with coverage is represented by scaling factors.

The line through the data points is actually the sum of the fitted components and demonstrates the quality of the fits. The spectra of the fresh cleave (labeled "clean") show the well-known decomposition into surface and bulk components.[24] The former, which accounts for about 30% of the total core level emission under surface sensitive conditions, results from the charge redistribution in the topmost layer, a consequence of the relaxation of the (110) surface. Up to a coverage of $\simeq 0.3$ Å, the spectra are basically only affected by band bending which is identical for both core levels. The spectra in Fig. 1 are from an *n*-type sample, the band bending shift is therefore directed toward higher kinetic energies. In addition, the components are slightly broadened with coverage, which is mainly due to inhomogeneities in band bending at submonolayer coverages. For coverages beyond $\simeq 0.3$ Å chemically shifted components become noticeable, which appear on the high kinetic energy side of both bulk components. This additional component is clearly observed in the Ga $3d$ spectra and becomes obvious when followed from higher to lower coverages. The chemically shifted component of the As $3d$ core level is not resolved for coverages lower than a few angstroms, as it partly overlaps the surface component, which appears, in contrast to the Ga $3d$ signal, on the high kinetic energy side of the bulk signal. The existence of a superimposed, chemically shifted component is nevertheless noticeable from both the broadening of what seems to be the As $3d$ surface component, which is not observed to that extent in the Ga $3d$ spectra, and from its absolute increase in integrated intensity, which is not expected for a pure surface component. With increasing coverage both core levels show increasing signal from the reacted components, which steadily shift to higher kinetic energies. For a coverage of about 5 Å (corresponding to $\simeq 2$ ML), the reacted components are of comparable intensity to the bulk signals, but dominate the spectra at 10 Å, the largest coverage for which the bulk components could be resolved. Beyond 10 Å (see Fig. 2), the As $3d$ signal is stronger attenuated than the Ga $3d$ signal, the latter still being present at a coverage of 35 Å. At this value the As $3d$ signal is just noticeable.

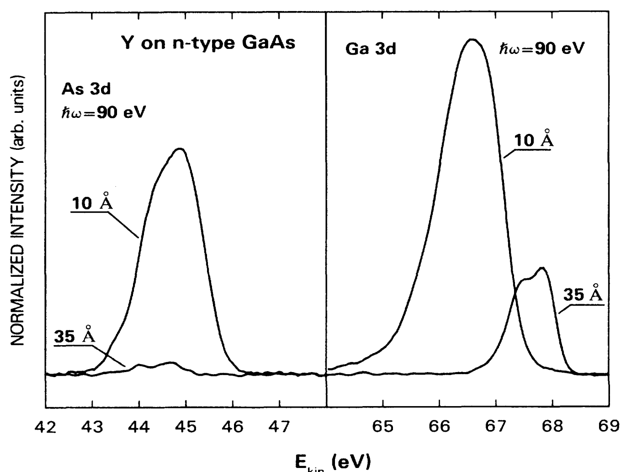

FIG. 2. Change in the Ga $3d$ and As $3d$ core levels between a coverage of 10 Å, which is characteristic for a heavily interacted interface, and a thick Y overlayer. The spectra are to scale and show the much stronger attenuation of the As $3d$ component compared to the Ga $3d$ signal. Note that only one sharp Ga component remains at 35 Å.

Additional information on the chemical surrounding of the reacted species can be derived from the lineshape of these signals: At coverages ≥ 1 Å, the reacted Ga $3d$ signal shows a pronounced asymmetry with a low-energy tail, which is indicative of many-body effects in the photoemission process, resulting from the dilution of Ga atoms or small Ga clusters in a metal environment.[11] Such asymmetries are well known from x-ray photoemission (XPS) spectra of metals,[25] and can to a good approximation be described by the analytical line shape given by Doniach and Šunjić (DS),[26] which was used in our fits for the chemically shifted Ga $3d$ component.

The shifted As $3d$ component, on the other hand, shows only a minor, if any, asymmetry (compare the two spectra at 10 Å coverage in Fig. 1). This finding together with the fact that the As $3d$ signal is more rapidly attenuated with increasing coverage suggests that reacted As atoms stay close to the interface in a predominately covalent or ionic local bonding environment, while Ga atoms diffuse into the growing Y film. Thus, the electron-hole pair creation near the Fermi edge, which is possible in a metallic environment and responsible for the DS line shape, is strongly suppressed in the case of the reacted As component, in sharp contrast to the core level signals of Ga atoms (or of small Ga clusters) diluted in the Y host.

Besides the different line shape of the reacted components, the full width at half maximum (FWHM) is in both cases very broad compared to the bulk signals. This broadening indicates a variety of different local chemical environments with slightly different binding energies, which cannot be resolved in the spectra and consequently appear as an increase of the Gaussian linewidth in our fitting routine. Such a strongly interacted layer is typical for the first few layers of transition metals on GaAs and has also been observed for Pd,[11] Ti,[11,27] V,[12,28] Mn,[12] Fe,[29] and Cr.[30] For all these cases one observes at higher coverages, when the supply of semiconductor species is diffusion limited, only one Ga $3d$ component, while one or two relatively sharp reacted components of the As $3d$ level survive. This applies also for Y and is illustrated in Fig. 2 for coverages of 10 and 35 Å. The intensity scale in Fig. 2 is identical for all four spectra and shows the strong attenuation of the As $3d$ signal. This is not the case for the other transition metals mentioned, which are characterized by Ga staying close to the interface and As diffusing into the growing film.

B. Fermi-level pinning

The spectral decomposition of the Ga $3d$ and As $3d$ core levels into bulk, surface and chemically shifted components allows one to monitor the Schottky-barrier formation by following the energetic position of the bulk components as a function of coverage. The resulting shift

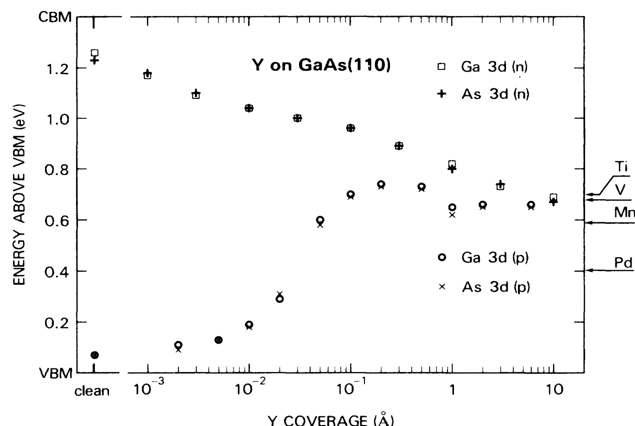

FIG. 3. Variation of E_F with respect to VBM as a function of Y coverage. The core-level shifts of the Ga $3d$ as well as of the As $3d$ bulk component are plotted. Note the pronounced differences in Fermi-level shift between n-type and p-type samples: While p-type GaAs becomes pinned at submonolayer coverages, n-type GaAs shows changes in E_F well into the metallic regime of the overlayer. Final pinning positions of other transition metals on GaAs (Refs. 11 and 12) are indicated on the right-hand side.

of the Fermi level at the interface with respect to the valence-band maximum (VBM) is plotted in Fig. 3 for n- and p-doped samples. The data points represent the relative shifts of the bulk component and are aligned with respect to the VBM, assuming flatband condition for the clean cleaved p-type sample. This results in a starting value of the Fermi-level 70 meV above VBM as calculated from the doping of our p-type samples. The assumption of flatband condition for the cleaved p-type sample is based on experimental observations on many cleaves, which for our samples showed that band bending was more likely to occur on n-type material. Nevertheless, we cannot completely rule out a small initial band bending on the p-type sample, which would result in a systematic error in the plotted Fermi-level positions. From comparisons with other cleaves, we estimate this error in the absolute energy values depicted in Fig. 3 to be less than 50 meV. The precision of the relative changes in the Fermi-level position is limited by the differences between the Ga $3d$ and As $3d$—derived band bending. As Fig. 3 shows, these differences are smaller than 50 meV for all coverages studied, even in the range beyond 1 Å, where the chemically shifted component complicates the Ga $3d$ spectra. This demonstrates that our fitting procedure is capable of separating the true bulk components with high precision, even in the case of a strongly interacted interface. Nevertheless, it has to be pointed out that the reaction products limit the maximum coverage for which the bulk component can be reliably extracted from the spectra to ≤ 10 Å ($\simeq 3$ ML). Similar limits have been found for other transition metals,[11,12] and appear to be typical for reacted overlayers, which do not show any tendency for clustering or island growth. The absence of cluster growth is clearly demonstrated by the small effective electron escape depth: From the attenuation of the Ga $3d$ and As $3d$ bulk components as a function of Y coverage, we derive a escape depth of 3 ± 0.5 Å in surface sensitive condition, which is comparable to the 2 ± 0.5 Å found for Ti overlayers.[11]

The variation of the Fermi-level pinning position as a function of Y coverages reveals a pronounced asymmetry between n- and p-type samples: While the Fermi-level shift for the p-type sample shows a relatively abrupt increase to within 100 meV of the final value in the coverage range between 0.01 and 0.1 Å, the n-type sample is characterized by a gradual shift over the entire, experimentally accessible coverage range. At 10 Å both samples reach the same pinning position in the band gap. Though the Fermi-level shift on n-type GaAs does not show a clear saturation behavior by then, we expect only minor changes at higher coverages once a metallic overlayer is formed, especially for the strongly reactive transition metals, which show no indication for clustering or island growth, as mentioned before. The latter growth mode is important for nonreactive systems like Ag on GaAs, where changes in the pinning position have been observed for coverages ≥ 20 ML.[23,31] However, the delayed pinning in such cases is attributed to lateral inhomogeneities in coverage (and consequently in pinning) rather than to intrinsic changes in the interface states.[23] A similarly delayed onset of the pinning has recently been observed for metals deposited at low temperatures.[32]

Although there may be small additional changes in Schottky-barrier height at higher coverages, which would require other techniques to be detected, the values reached within the coverage range accessible by PES experiments already allow a comparison between different transition-metal overlayers. For that purpose we marked on the right-hand ordinate in Fig. 3 the Fermi-level pinning positions for several transition metals reached at comparable coverages. These pinning positions, which are spread over a range of about 300 meV within the bandgap, are discussed together with the apparent differences in interface chemistry in Sec. III.

C. Valence-band studies

In addition to core-level studies, which give information about the interface chemistry and the band bending, we also performed valence band studies of filled and empty states to obtain further insight into the possible Schottky-barrier formation processes. Figure 4 shows valence band photoemission spectra of an n-GaAs sample for several Y coverages at a photon energy of 90 eV. The abscissa is scaled in energy relative to the Fermi level, i.e., the raw data in the left panel show the changes in valence band emission including the band-bending shift. The intensities for the different coverages are not to scale so as to reveal details at low coverages. The raw data are complemented by difference spectra on the right-hand side, which depict the spectra at the indicated coverages after subtraction of the clean spectrum. For this purpose, the two respective spectra have been corrected by the band bending shift derived from the substrate core-level signals and aligned in intensity by scaling to the low-energy feature in the valence band. The scaling works quite well

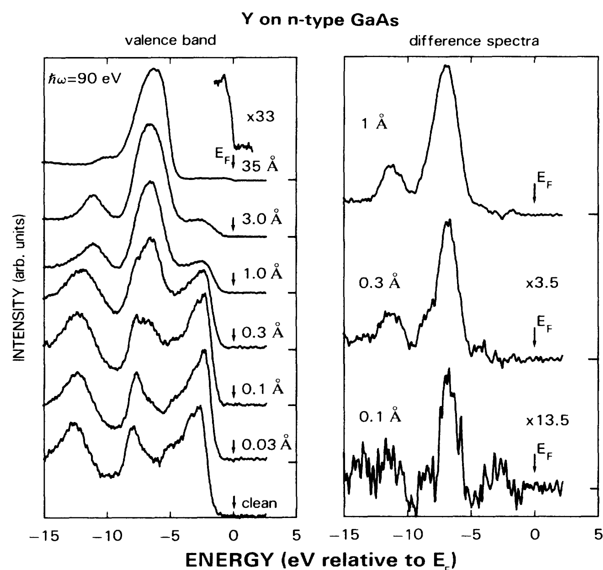

FIG. 4. Development of the valence-band PES spectra upon Y deposition. In addition to the raw data in the left panel, difference spectra between the spectra at the noted coverages and the clean spectrum are plotted in the right frame. Intensities are not to scale to reveal details at low coverages. The spectrum at 35 Å is typical for an Y film and shows the mainly s-electron-derived Fermi edge in the enlarged section. Additional emission from the Y d electron becomes visible from 0.03 Å on and is located about 7 eV below E_F.

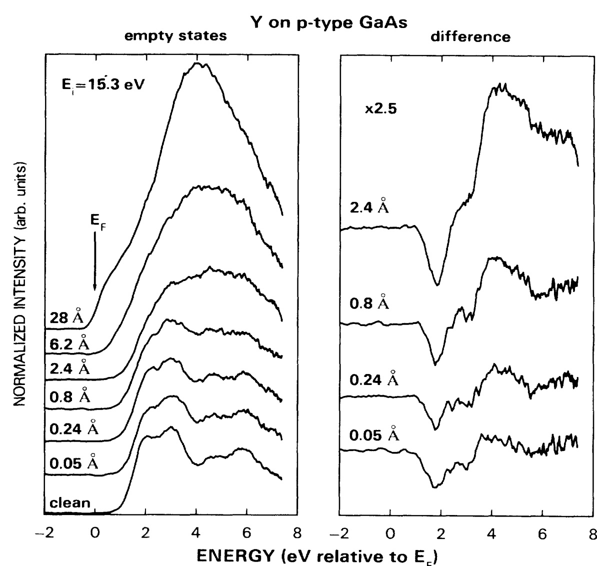

FIG. 5. Normal emission IPES raw and difference spectra for various Y coverages. All spectra are normalized to the electron flux. The appearance of the empty Y $4d$ states at eV above E_F, concomitant with the loss of a surface state at the conduction-band onset can be followed down to the lowest Y coverage. The broad $4d$ signal tails into the band-gap region at coverages above 2 Å, indicating the beginning formation of a metallic overlayer.

for Y coverages below 1 Å, but the raw data in the left panel indicate a shift of the lowest valence band peak toward higher energies, which makes a proper alignment somewhat ambiguous at higher coverages. The observed shift itself is not unexpected, since the lowest valence band peak is mainly derived from As $4s$ orbitals and is therefore strongly affected by the presence of a reacted As species at the interface. Consequently, the shift of that peak follows closely the energetic position of the reacted As $3d$ component (compare Fig. 1).

The raw data, and more clearly the difference spectra, show emission from the Y $4d$ level for coverages as low as 0.1 Å (0.03 ML), which appears around 7 eV below the Fermi level, developing successively to the dominating valence-band feature with increasing coverage. An additional peak appears in the difference spectra at $\simeq$11 eV below E_f, which results from the mentioned shift of the As $4s$—derived valence-band feature. The topmost spectrum at $\simeq$35 Å is characteristic for metallic Y and shows in the enlarged section the Fermi edge, made up predominately from s electrons. There is no indication either in the raw data or in the difference spectra for additional emission in the band gap region up to coverages of several angstroms, at which value the Fermi edge of the truly metallic overlayer becomes observable.

The variations in the density profile of empty states above E_f as a function of Y coverages are shown in Fig. 5. The IPES spectra were taken in normal emission ($k_{\parallel}=0$) at an electron energy of 15.3 eV. The raw data in the left panel are normalized to the electron flux; the right panel shows difference spectra between the respective spectrum at the indicated coverage and the clean spectrum. The evolution of the raw data, and more pronounced the difference spectra, show the development of the empty d states as a broad peak at 4 eV above E_f. The other major change is the disappearance of the relatively sharp feature at the conduction band onset of the clean surface, which is attributed to a surface state. This effect becomes visible in the difference spectra as a dip around 2 eV, and partly obscures the tail of the d-related signal that extends into the band gap with increasing coverage. This tail is clearly visible at the two highest coverages studied. The final spectrum at 28 Å ($\simeq$10 ML) shows a distinct cutoff at the position of the Fermi level, indicating that the Y overlayer has bulk character by then. Nevertheless, the spectra do not show evidence for empty states in the bandgap for coverages below 2 Å.

It is obvious from the PES and IPES experiments that the filled and empty states created by the Y d levels do not overlap the intrinsic band-gap region of GaAs at low coverages, but appear several eV inside the valence and conduction band, respectively. Emission within the band gap becomes visible after the overlayer has metallic character. This behavior is substantially different from other transition metals studied recently, which show filled and empty states within the band gap at coverages much below one monolayer, i.e., before the overlayer can develop metallic properties. This is demonstrated in Fig.

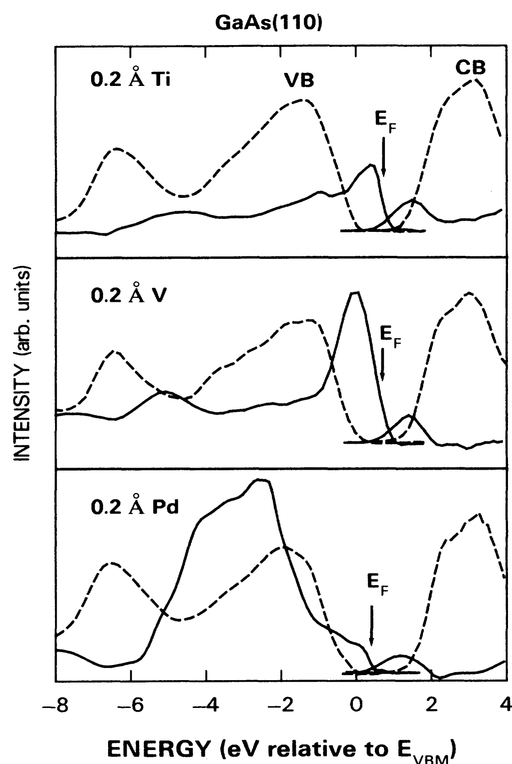

FIG. 6. In contrast to Y, other transition metals show filled and empty d-electron-related states in the band gap at coverages well below the onset of metallic properties. Ti, V, and Pd data are shown as examples. The plots combine photoemission and inverse-photoemission spectra of clean samples (dashed) and difference spectra at coverages of 0.2 Å of the respective metal.

6, which depicts the additional filled and empty states in the vicinity of the band gap induced by small amounts of Ti, V, and Pd deposited on cleaved GaAs samples (solid lines). The dashed curves show the valence and conduction bands as derived from PES and IPES experiments on clean cleaves. The d-derived bandgap states extend in all three cases up to the Fermi level, providing strong evidence for their direct involvement in the pinning process.

III. DISCUSSION

The experimental results presented in the preceding section reveal pronounced differences in the chemical and electronic behavior of Y on GaAs with respect to other $3d$ and $4d$ transition metals. As far as chemistry is concerned, the predominant outdiffusion of Ga rather than As into the metal overlayer has not been observed for the $3d$ and $4d$ transition metals studied so far. The line shape of the reacted As $3d$ compound indicates a strong bond between As and Y atoms, which is consistent with the large electronegativity difference of the two species: Y has, with a value of 1.2,[33] the lowest electronegativity of all $3d$ and $4d$ transition metals, which is substantially lower than that of As (2.0) and also less than the value for Ga(1.5). In contrast, the other transition metals that have been studied (V, Ti, Cr, Mn, Fe, and Pd) have electronegativities comparable to that of Ga. This suggests that the interface reactions consist basically in the formation of Y—As bonds, which releases Ga atoms from their lattice sites. The reaction at this stage is not stoichiometric, as can be seen in the inhomogeneous broadening of the reacted Ga and As core levels, and most likely affects several atomic layers of the substrate. The observed shift of the reacted As $3d$ component toward higher kinetic energy results from a charge transfer from Y atoms, as expected from the large electronegativity difference. This effect becomes also visible in the shift of the As $4s$ derived valence-band feature that has been mentioned above (see Fig. 4). The Ga atoms released in the earlier stages of the interface reaction diffuse into the Y overlayer, probably forming an alloy, which becomes more and more Y rich with increasing thickness of the overlayer, as the interacted layer forms an effective barrier for further out diffusion of Ga atoms. The final stage is reached when isolated Ga atoms are surrounded by a local Y environment, resulting in a Ga $3d$ spectrum consisting of only one sharp peak (see Fig. 2).

The simplified description of the likely reactions at the Y-GaAs interface is based on the observed changes in the core-level spectra and the differences in electronegativity. The use of electronegativity seems to be justified for the present case, and is supported by recent experiments at the interface between the $4f$ metal Yb and GaAs:[34] Yb has a comparable small electronegativity of 1.1, and shows a similar reaction kinetic at the interface as Y, i.e., Ga diffuses into the overlayer while As stays close to the interface. On the other hand, care has to be taken when the electronegativity differences between the reacting species are small, as is the case with most other transition metals on GaAs: Although a cation replacement reaction is the most probable initial reaction for all of these interfaces, it is at present not understood, why for those systems the cation stays close to the interface upon further metal deposition while the anion diffuses into the overlayer.

The other interesting aspect of the Y-GaAs system, namely the electronic properties of the interface, differs also substantially from the behavior found with other transition-metal—GaAs interfaces: From the simple counting of the valence electrons, mentioned in Sec. I, it is clear that no d-electron-related filled states of Y atoms at a substitutional cation site are expected to overlap the intrinsic bandgap region. This expectation is confirmed by the PES experiments, which are consistent with the assumption of a cation replacement reaction, but also reveal that the filled d state is located several eV below E_F. Nevertheless, we observe a Schottky barrier of 0.68 ± 0.05 eV on p-type, and of 0.73 ± 0.05 eV on n-type GaAs, close to the barrier heights found with V and Ti overlayers. The latter two metals show a large density of filled and empty, d-electron-related states at the Fermi level at coverages long before the overlayer becomes metallic (see Fig. 6). This finding together with the known donor and acceptor properties of these metals in bulk samples led us to the conclusion that the rehybridized d orbitals provide the dominating mechanism for the observed Schottky-barrier

formation.[11,12] The same argument applies for Pd (Ref. 11) and to some extent also for Mn,[12] but the lack of *d*-electron-related band-gap emission in the present case of Y rules out the involvement of *d* orbitals in the pinning mechanism for *p*-type GaAs. The situation is not so clear cut for *n*-type GaAs, which is characterized by a gradual shift of the Fermi level toward the final pinning position: About 40% of the total band bending occurs in a coverage range beyond 0.1 Å, where chemical reactions and tailing of the predominately *d*-like empty states into the intrinsic bandgap become visible in the experiments. In contrast, the Fermi level on *p*- GaAs lies within 100 meV of the final pinning position already at a coverage of 0.1 Å. This pronounced asymmetry in Schottky-barrier formation suggests different mechanisms being responsible for the creation and energetic distribution of donor and acceptor states at the Y-GaAs interface. The following discussion will therefore treat the pinning on *n*- and *p*-type samples separately.

The *p*-type GaAs-Y interface reaches its final pinning position at very low coverages with only minute changes in the regime of strong chemical reactions at the interface and the eventual development of a metallic overlayer. The results suggest that the energetic distribution of donors created upon deposition of about 0.1 Å Y is almost unaffected by the subsequent interface chemistry and the screening properties of a true metal overlayer. This implies that either a high density of donors of the order of 10^{14} cm^{-2} has been created at 0.1-Å coverage, or that the same kind of donor states is also produced in the reaction regime. In either case, it is expected that some 10^{14} cm^{-2} donors are present at several-angstrom coverage, when the overlayer becomes metallic. Otherwise, the metallic screening properties would affect the final pinning position according to recent theoretical results.[35,36]

The experiments do not provide direct access to the origin of the donor states created upon Y deposition on *p*-type GaAs: As the experiments lack any evidence for filled gap states in the low coverage range, the Y-GaAs interface resembles the situation found for most of the simple, nontransition metals, where surface donor states also escaped detection in photoemission experiments, either because of the small density of those states or, more likely, because of their small photoemission cross section. Nevertheless, the observed interface chemistry and the pinning behavior allow to select some potential mechanisms, which will be briefly discussed in the following.

The reactivity of Y that is observed in the core-level spectra and the local inhomogeneities inside the reacted layer, which lead to a broadening of the reacted Ga 3*d* and As 3*d* components, suggest that besides substitutional cation impurities other kinds of defects, e.g., vacancies or ternary complexes, are created during the first phase of Y deposition. It is well known from calculations that filled and empty electron levels associated with such defects can be located within the intrinsic gap of GaAs, and therefore can contribute to the Schottky-barrier formation.[37] These theoretical results were important for the formulation of the so called "unified defect model" (UDM), which attributes the Schottky-barrier formation to a universal pair of GaAs-derived defects that are created during the first steps of metal deposition: Ga and As vacancies, or As_{Ga} and Ga_{As} antisite defects have been named as candidates for donor and acceptor states, respectively.[38,39] Despite recent modifications that reduce some of the early shortcomings of the UDM,[5] such as the prediction of two different pinning levels for *n*- and *p*-type semiconductors, the main problem remains the experimental identification of the proposed defects. Moreover, the claimed universality of the model has been questioned by recent experiments on the Ge-GaAs interface,[40,41] which revealed Fermi-level pinning only in the case of an amorphous, but not for an epitaxial Ge overlayer.[40] This finding is hard to reconcile with the UDM, as it appears unlikely that native GaAs defects should only be created at low-temperature deposition of Ge, which leads to an amorphous overlayer, but not under epitaxial growth conditions. The interpretation given in Ref. 40 attributes the pinning behavior for the amorphous overlayer to Ga and As dangling bonds at the interface that are not saturated by Ge bonds because of local disorder in the amorphous film. This mechanism is more satisfactory than one based on intrinsic GaAs defects and might also be important for the present case of a heavily reacted overlayer.

Another possible source of interface states is related to the cation replacement reaction, which we identified as the most likely initial reaction upon Y deposition. At submonolayer coverages the released Ga atoms have to stay at the surface, before a part of them can be successively incorporated into the growing Y film during further Y deposition. The early Y-adsorption regime resembles therefore models that have been proposed for low-coverage Al-GaAs interfaces,[42] where a corresponding Al-Ga replacement reaction was assumed. As neither Al nor Y at a cation site of the surface create intrinsic donor states, it is conceivable that the observed band bending in both cases is due to the replaced Ga atoms. This argument is supported by the fact that the Ga-GaAs interface is also pinned.[43] Unfortunately, no high-resolution band bending studies are available for low Ga coverages (≤ 0.1 Å), which would be necessary to test if a predominant creation of donors at the Y-GaAs interface can be related to an energetically favorable binding site of replaced Ga atoms at the surface, as is suggested by energy-minimization calculations.[44] At higher coverages, however, the possible similarity between the Y-GaAs and the Ga-GaAs interface is no longer expected. Ga (like other column III atoms) clusters at room temperature, an effect which is unlikely in the present case because of the relatively small amount of Ga atoms released and its alloy formation with the Y overlayer. Hence, the experimental finding that Ga pins both *n*- and *p*-type GaAs at coverages >1 Å (Ref. 43) does not rule out the possibility of a predominant donor creation at submonolayer coverage. Certainly, additional experiments of the Ga-GaAs interface, preferentially performed at low temperatures in order to suppress cluster formation, are necessary to substantiate the relevance of this pinning mechanism.

As mentioned above, the *n*-type GaAs-Y interface behaves in a substantially different manner as far as Schottky-barrier formation is concerned: Although we observe band bending from the lowest Y coverage on, the

final barrier height is not established before the overlayer is truly metallic. The gradual shift of the Fermi level over such a large coverage range has so far only been observed for metal overlayers that form clusters or islands upon room-temperature deposition. Such a growth mode definitely does not apply to the Y-GaAs interface (compare Sec. II B). A simple interpretation in terms of lateral inhomogeneous band bending is therefore inadequate for the present system, especially as *p*-type GaAs would be affected as well, which is obviously not the case. The *n*-type GaAs-Y interface appears to be much more complicated and most likely has several pinning mechanisms involved. At low coverages donor as well as acceptor states are produced, since both *n*- and *p*-type substrates show band bending from the smallest Y depositions on. Any of the three mechanisms discussed above as sources for donor creation can in principle also be associated with acceptor production. However, it appears unlikely that the defect mechanism of the UDM is applicable here, as it assumes an acceptor level far down in the band gap, which does not correspond to the shallow barrier on *n*-type GaAs reached at low coverages. In order to fit the UDM to the Y-GaAs interface, one has to assume that the density of acceptors is too small to pin the Fermi level at low coverages. This means that the rate for acceptor production would have to be much smaller than the one for donors, which is not supported by experiments on other systems that have been described in terms of the UDM. The second mechanism, namely the donor and acceptor properties of unsaturated dangling bonds at the interface, is based on *n*-type GaAs-Ge interfaces only[39] and needs confirmation on *p*-type substrates before its relevance for the present interface can be judged. More experiments are also necessary for the third proposed mechanism, which is related to the role of released Ga atoms at the interface. It is however worth noting that energy-minimization calculations show several energetically favorable binding sites of Ga atoms on the GaAs(110) surface, which differ somewhat in binding energy.[42] These sites affect also the associated density of states in the bandgap, i.e., they can have donor or acceptor properties. The energy difference between two such sites would then determine the probability of their occupation by released Ga atoms and might account for a much smaller density of acceptors, which is too low to pin the Fermi level at submonolayer coverages. In addition, the simple acceptor state might be close to the conduction band, accounting for the shallow barrier found at low coverges at the *n*-type GaAs-Y interface.

Whatever the acceptor-creating mechanisms at low coverages are, the delayed formation of the Schottky barrier suggests that other mechanisms contribute in the interaction regime. From the low-coverages IPES spectra, we can exclude that empty *d*-derived states associated most likely with a cation replacement reaction provide a source for acceptors, since such states appear several eV in the conduction band. With increasing coverage, however, the overlayer gradually develops metallic band structure, which is characterized by tailing of the empty states toward the Fermi level. Although such a tailing does not become obvious in the IPES spectra at Y coverages below 2 Å, an earlier onset of a gradual overlap between the metal density of states and the semiconductor band gap appears plausible: A small density of states would most likely escape experimental detection, as the scattering cross section for *d*-like states at an electron energy of 15.3 eV used in the IPES measurements is much smaller than the one in the PES experiments, which were performed at a photon energy of 90 eV. Another problem is the disappearance of a pronounced surface resonance in the IPES spectra, which affects the conduction band onset of the clean spectrum. This leads to the negative peak in the difference spectra of Fig. 5, which could easily disguise an early tailing of the empty *d* states into the intrinsic band gap.

The gradual development of metal-derived states, which move downward with increasing coverage, could provide a source for acceptorlike density of states that changes its energetic position with increasing overlayer thickness. Such a mechanism appears interesting, especially in connection with a class of models, which are based on metal-induced gap states (MIGS) as a potential source for Fermi-level pinning.[1–4] Such models are usually calculated for abrupt interfaces between semiconductors and metallic overlayers, but it is clear that the metal band structure develops gradually under experimental conditions. Nevertheless, it appears impossible, to extract such an effect in a quantitative way from our experiments, since we cannot entirely rule out the generation of localized acceptor states at lower energies in the interaction regime, which could as well account for the observed gradual shift of the Fermi level. Hence, lacking an experimental technique that provides information about the exact distribution of acceptor and donor states in the band gap as a function of coverage, we can only speculate about the potential influence of MIGS. However, it should be pointed out that even if MIGS play a role in pinning the Fermi level at the *n*-type GaAs-Y interface, their efficiency is obviously very limited and their effect can easily be overruled by a high density of localized interface states: This is observed for the *p*-type GaAs-Y interface as well as for the transition metals in Fig. 6, which all show pinning close to the saturation value at very low coverages.

In summary, we have studied the Y-GaAs interface, which shows several unusual features as compared to other transition-metal—GaAs systems. Though the interface is heavily reacted, like with other $3d$ and $4d$ metals, the small electronegativity of Y compared to Ga and As leads to a strong bond between As and Y and drives substituted Ga atoms into the growing metal film. In contrast, other transition metals studied recently reveal a more complex interface chemistry, which is most likely also started by Ga substitution, but subsequently results in outdiffusion of As into the overlayer.

Besides the interface chemistry, the most remarkable finding is the Schottky-barrier formation, especially the pronounced differences between *n*- and *p*-type GaAs: *p*-type GaAs is characterized by Fermi-level pinning at submonolayer coverages, while the Schottky-barrier formation on *n*-type GaAs extends into a coverage range where the overlayer becomes metallic. This means that at low coverages mainly donor states are created at the interface, while the density or the initial energetic distribution of ac-

ceptor states is not sufficient to pin the Fermi level at its final position. The origin of the surface donors is not understood yet, but we can rule out that rehybridized *d* electrons, which most likely provide donor states in several other transition-metal—GaAs systems, are involved in the Fermi-level pinning at the Y—*p*-type-GaAs interface. Empty *d*-derived states might play a role as acceptor states in the intermediate coverage regime, but this effect, if it exists, results from the properties of the Y overlayer and not from the empty levels associated with a simple substitutional defect.

The results of the Y-GaAs interface show that we are still far from understanding the basic, microscopic mechanisms that lead to the formation of a Schottky barrier. The future development in this field will strongly depend on new spectroscopic methods, which hopefully allow a positive identification of the interface states created at submonolayer coverages, and on the ability for a reasonable description of the intermediate coverage range between interface creation and metallic screening.

ACKNOWLEDGMENTS

We thank M. Prikas for his expert help in preparing the experiments and the staff of the National Synchrotron Light Source (NSLS) at Brookhaven National Laboratory for their technical assistance. This work was partially supported by the U. S. Army Research Office under Contract No. DAAG-29-83-C-0026.

---

*Present address: School for Physical Sciences, NIHE, Glasnevin, Dublin 9, Ireland.

[1]V. Heine, Phys. Rev. **138A**, 1689 (1965).

[2]S. G. Louie and M. L. Cohen, Phys. Rev. B **13**, 2461 (1976).

[3]C. Tejedor, F. Flores, and E. Louis, J. Phys. C **10**, 2163 (1977).

[4]J. Tersoff, J. Vac. Sci. Technol. B **3**, 1157 (1985), and references therein.

[5]W. E. Spicer, T. Kendelewicz, N. Newman, K. K. Chin, and I. Lindau, Surf. Sci. **168**, 240 (1986), and references therein.

[6]L. J. Brillson, Surf. Sci. Rep. **2**, 123 (1982), and references therein.

[7]J. L. Freeouf and J. M. Woodall, Appl. Phys. Lett. **39**, 727 (1981).

[8]A. Nedoluha, J. Vac. Sci. Technol. **21**, 429 (1982).

[9]R. Haight and J. Bokor, Phys. Rev. Lett. **56**, 2846 (1986).

[10]R. E. Viturro, M. L. Slade, and L. J. Brillson, Phys. Rev. Lett. **57**, 487.

[11]R. Ludeke and G. Landgren, Phys. Rev. B **33**, 5526 (1986).

[12]G. Hughes, R. Ludeke, F. Schäffler, and D. Rieger, J. Vac. Sci. Technol. B **4**, 924 (1986).

[13]H. Katayama-Yoshida and A. Zunger, Phys. Rev. B **31**, 7877 (1985); **33**, 2961 (1986).

[14]M. J. Caldas, S. K. Figueiredo, and F. Fazzio, Phys. Rev. B **33**, 7102 (1986), and references therein.

[15]A. M. Hennel, C. D. Brandt, Y.-T. Wu, T. Bryskiewicz, K. Y. Ko, J. Lagowski, and H. C. Gatos, Phys. Rev. B **33**, 7353 (1986).

[16]U. Kaufmann, J. Schneider, Festkörperprobleme, Advances in Solid State Physics, edited by J. Treusch (Vieweg, Braunschweig, 1980), Vol. XX, p. 87.

[17]B. Clerjaud, J. Phys. C **18**, 3615 (1985) and references herein.

[18]F. Schäffler, W. Drube, G. Hughes, R. Ludeke, D. Rieger, and F. J. Himpsel, Proceedings 10th International Conference on Solid Surfaces [J. Vac. Sci. Technol. A (to be published.)]

[19]R. Ludeke, D. Straub, F. J. Himpsel, and G. Landgren, J. Vac. Sci. Technol. A **4**, 874 (1986).

[20]R. Ludeke, G. Hughes, W. Drube, F. J. Himpsel, F. Schäffler, D. Rieger, D. Straub, and G. Landgren (unpublished).

[21]D. E. Eastmann, J. J. Donelon, N. C. Hien, F. J. Himpsel, Nucl. Instrum. Methods **172**, 327 (1980); F. J. Himpsel, Y. Jugnet, D. E. Eastman, J. J. Donelon, D. Grimm, G. Landgren, A. Marx, J. F. Morar, C. Oden, R. A. Pollak, J. Schneir, and C. A. Crider, *ibid.* **222**, 107 (1984).

[22]T. Fauster, D. Straub, J. J. Donelon, D. Grimm, A. Marx, and F. J. Himpsel, Rev. Sci. Instrum. **56**, 1212 (1985).

[23]R. Ludeke, Surf. Sci. **168**, 290 (1986).

[24]D. E. Eastman, T.-C. Chiang, P. Heimann, and F. J. Himpsel, Phys. Rev. Lett. **45**, 656 (1980).

[25]G. K. Wertheim, P. H. Citrin, *Photoemission in Solids I*, edited by M. Cardona and L. Ley (Springer-Verlag, Berlin, 1978).

[26]S. Doniach and M. Šunjićc, J. Phys. C **3**, 285 (1970).

[27]M. W. Ruckman, M. del Giudice, J. J. Joyce, and J. H. Weaver, Phys. Rev. B **33**, 2191 (1986).

[28]M. Grioni, J. J. Joyce, and J. H. Weaver, J. Vac. Sci. Technol. A **3**, 918 (1985).

[29]M. W. Ruckman, J. J. Joyce, and J. H. Weaver, Phys. Rev. B **33**, 7029 (1986).

[30]J. H. Weaver, M. Grioni, and J. J. Joyce, Phys. Rev. B **31**, 5348 (1985).

[31]F. Schäffler and G. Abstreiter, J. Vac. Sci. Technol. B **3**, 1184 (1985).

[32]K. Stiles, A. Kahn, D. Kilday, N. Tache, and G. Margaritondo, J. Vac. Sci. Technol. (to be published).

[33]All electronegativity values are taken from W. Gordy and W. J. O. Thomas, J. Chem. Phys. **24**, 439 (1955).

[34]J. Nogami, M. D. Williams, T. Kendelewicz, I. Lindau, and W. E. Spicer, J. Vac. Sci. Technol. A **4**, 808 (1986).

[35]A. Zur, T. C. McGill, and D. L. Smith, Phys. Rev. B **28**, 2060 (1983).

[36]C. B. Duke and C. Mailhoit, J. Vac. Sci. Technol. B **3**, 1170 (1985).

[37]R. E. Allen and J. D. Dow, Phys. Rev. B **25**, 1423 (1982).

[38]W. E. Spicer, P. W. Chye, P. R. Skeath, C. Y. Su, and I. Lindau, J. Vac. Sci. Technol. **16**, 1422 (1979).

[39]W. E. Spicer, I. Lindau, P. Skeath, C. Y. Su, and P. Chye, Phys. Rev. Lett. **44**, 420 (1980).

[40]H. Brugger, F. Schäffler, and G. Abstreiter, Phys. Rev. Lett. **52**, 141, (1984).

[41]P. Chiaradia, A. D. Katnani, H. W. Sang, Jr., and R. S. Bauer, Phys. Rev. Lett. **52**, 1246 (1984).

[42]J. Ihm and J. D. Joannopoulos, Phys. Rev. B **26**, 4429 (1982).

[43]P. Skeath, I. Lindau, P. W. Chye, C. Y. Su, and W. E. Spicer, J. Vac. Sci. Technol. **16**, 1143 (1979).

[44]D. J. Chadi and R. Z. Bachrach, J. Vac. Sci. Technol. **16**, 1159 (1982).